Received: 25 May 2021 | Revised: 20 December 2021 | Accepted: 22 December 2021

DOI: 10.1002/eco.2399

RESEARCH ARTICLE

WILEY

Water conservation potential of modified turf grass irrigation in urban parks of Phoenix, Arizona

Mercedes Kindler[1] | Enrique R. Vivoni[1,2] | Eli R. Pérez-Ruiz[2,3] | Zhaocheng Wang[1]

[1]School of Sustainable Engineering and the Built Environment, Arizona State University, Tempe, Arizona, USA

[2]School of Earth and Space Exploration, Arizona State University, Tempe, Arizona, USA

[3]Departamento de Ingeniería Civil y Ambiental, Universidad Autónoma de Ciudad Juárez, Ciudad Juárez, Mexico

Correspondence
Enrique R. Vivoni, School of Earth and Space Exploration, Arizona State University, Tempe, AZ 85287-6004, USA.
Email: vivoni@asu.edu

Funding information
Metropolitan Water District of Southern California; City of Phoenix; Central Arizona Project

Abstract

Large amounts of water are consumed by urban parks in arid regions such that efficient irrigation practices are needed. In Phoenix, Arizona, extensive turf grass areas are supported using flood or sprinkler irrigation that also require fertilizers. Residential green waste compost has the potential to serve an alternative fertilizer if its higher costs can be offset through water conservation. In this study, we conducted an ecohydrological monitoring and modelling effort for a compost experiment in two urban parks with either flood or sprinkler irrigation. Soil moisture, evapotranspiration and turf greenness data along with a soil water balance model were used to determine if compost treated plots were different from control plots in each park. After building confidence in the model through comparisons to data, we created long-term scenarios to explore differences between flood and sprinkler irrigation practices and analyse the effect of changes in irrigation scheduling. Multiple lines of evidence indicated that green waste compost applications did not appreciably change soil moisture or vegetation conditions in either urban park. Major differences, however, were noted between the two irrigation practices in terms of the seasonality of the soil water balance, plant water stress and the sensitivity to interannual fluctuations in precipitation. Model scenarios showed that significant irrigation reductions from 15% to 30% could be achieved, in particular with small changes in watering depths. As a result, irrigation management in urban parks can meet water conservation targets that potentially offset green waste compost costs while also benefitting the soil water balance through reductions in water losses.

KEYWORDS
circular economy, compost, evapotranspiration, modelling, outdoor water use, plant water stress, soil water balance, urban ecohydrology

1 | INTRODUCTION

The Southwestern United States is a hot and arid region with a population that is expected to grow by ~70% by mid-21st century, which could potentially lead to additional water stress (Garfin et al., 2014; McDonald, 2010). While most of the water in the region is used by agriculture, a considerable and growing amount is consumed by green infrastructure in urban areas (Gleick, 2010; Pataki et al., 2011) such that efficient outdoor water use practices are needed. Prior studies suggest that urban irrigation approaches that account for climate, soil conditions and vegetation requirements could potentially lead to water conservation (Quesnel et al., 2019; Volo et al., 2014; Volo et al., 2015). However, water conservation might also negatively impact a multitude of beneficial ecosystem services

provided by green areas, including heat amelioration, aesthetics, recreational use and property values (e.g., Beard & Green, 1994; Gober et al., 2010; Larson & Perrings, 2013; Vivoni et al., 2020; Yabiku et al., 2008). As a result, reductions in outdoor water use need to be considered in light of other constraints on residents, community organizations and municipal agencies that manage urban irrigation (e.g., Grimm et al., 2008; Wang, Turner, et al., 2021).

In the City of Phoenix, Arizona, 40% to 88% of residential water use may be applied towards outdoor landscaping (Balling et al., 2008), with a large proportion used for maintaining non-native plants such as turf grasses that are typically arranged with a few trees (e.g., Hirt et al., 2008; Larson et al., 2009; Templeton et al., 2018). While per capita water use in Phoenix has been reduced by ~15% from 1980 to 2005 through conservation programmes, outdoor use remains high (Balling & Gober, 2007), partly since irrigation is rarely adjusted in response to weather conditions (Martin, 2008). In Phoenix, warm season turfs composed of perennial grasses, such as bermudagrass (*Cynodon dactylon*), are maintained through either flood or sprinkler irrigation practices (Brown et al., 2001). The selection of irrigation type depends on a number of factors, including historical legacies, infrastructure and resident choices (Larson et al., 2017), and have been shown through modelling to have a strong influence on the components of the soil water balance (Volo et al., 2014). In particular, changes to irrigation amounts or frequency have the potential for conserving outdoor water use, while minimizing impacts to turf grass health.

In addition to substantial watering, warm season turf grasses require the use of fertilizers that are often sourced from manufactured chemicals (e.g., Milesi et al., 2005; Robbins & Sharp, 2003). More recently, there has been a growing interest in using residential green waste compost as an alternative. This is attractive in Phoenix due to the substantial amounts of plant trimmings generated in residential yards, common areas, and parks (Martin, 2008). In response, the City of Phoenix invested in composting facilities (Coker, 2017) whose products are a potential fertilizer source for urban parks and for other markets within a circular economy paradigm (Buch et al., 2018). In addition to a lower use of traditional fertilizers, the application of green waste compost in turf grass areas might provide the additional benefit of conserving soil water, as prior studies have identified this potential under certain conditions (Weindorf et al., 2006; Zemánek, 2011). Nevertheless, the efficacy of this alternative fertilization strategy in urban park settings has yet to be established for different types of irrigation practices.

In this study, we conducted an ecohydrological monitoring and modelling effort in the context of a compost experiment in two urban parks with representative flood and sprinkler irrigation practices in Phoenix, Arizona. Soil moisture and turf grass observations along with a physically based soil water balance model were used to determine if compost treated plots were different from control plots. After calibrating and testing the model against soil moisture and evapotranspiration data, we analysed a series of long-term scenarios to determine the water conservation potential of modified irrigation schedules. Alternative scenarios were designed based on a water reduction target linked to the economic viability of green waste compost and subsequently assessed based on the simulated water balance components and turf grass stress. Throughout the effort, a close coordination with the City of Phoenix Parks and Recreation Department allowed for placing the data analyses and modelling scenarios in a real-world management context and providing solutions tailored to the challenges faced by practitioners to promote their adoption. We expect this study will yield insights on the utility of green waste compost and alternative irrigation scheduling for urban water conservation and thereby inform other circular economy efforts. This work also illustrates how observational and modelling approaches can be integrated with experimental manipulations in urban settings to study ecohydrological processes that are driven by management decisions.

2 | STUDY SITES

Two urban parks were selected based on their varying types of irrigation and the prior establishment of control and treatment plots for compost additions. Paradise Valley Park (PV) in north Phoenix has a large turf grass area that receives sprinkler irrigation, while Encanto Park (EN) in central Phoenix receives flood irrigation within turf grass areas next to the historical Norton House (Figure 1). Table 1 provides the general characteristics of each study park. Both sites contain a few shade trees but are primarily covered by bermudagrass maintained by the Parks and Recreation Department of the City of Phoenix. At both parks, control (C) plots with no compost additions were situated near compost treatment (T) plots that received green waste compost twice per year in the fall and spring from 2015 to 2019. For each date, ~0.6-cm-depth compost was applied as a top-dressing and incorporated into the turf grass surface with a drag mat. Turf grass at the study parks experienced two main seasons: (1) an active growing period (or 'Warm Season', defined here as 1 April to 30 September) with warm temperatures, frequent irrigation and high lawn maintenance and (2) a dormant period (or 'Cool Season', 1 October to 31 March) with cooler temperatures, less frequent irrigation and lower mowing requirements.

Both study parks have relatively flat topography due to their locations on an alluvial fan surface (0 to 3% slope at PV) and an alluvial plain (0 to 1% slope at EN), with well-drained soils of loamy texture (Table 1, Gilman and Mohall series at PV and EN, respectively). Initial construction and several decades of soil and water treatments have modified conditions at both sites, in particular at EN where plots are below-grade to allow for flood inundation. Climate at the parks is classified as hot desert (Köppen BWh) with a low average annual precipitation (P) of 190 mm/year, as measured at Phoenix Sky Harbor Airport (1950–2018, Templeton et al., 2018). As shown in Table 2, a bimodal regime leads to higher amounts of precipitation in the cool season as compared to the warm season, though interannual variability in seasonal precipitation is large (Mascaro, 2017). Weather data at each park were monitored through nearby stations from the Arizona Meteorological Network (AZMET, Desert Ridge and Phoenix Encanto

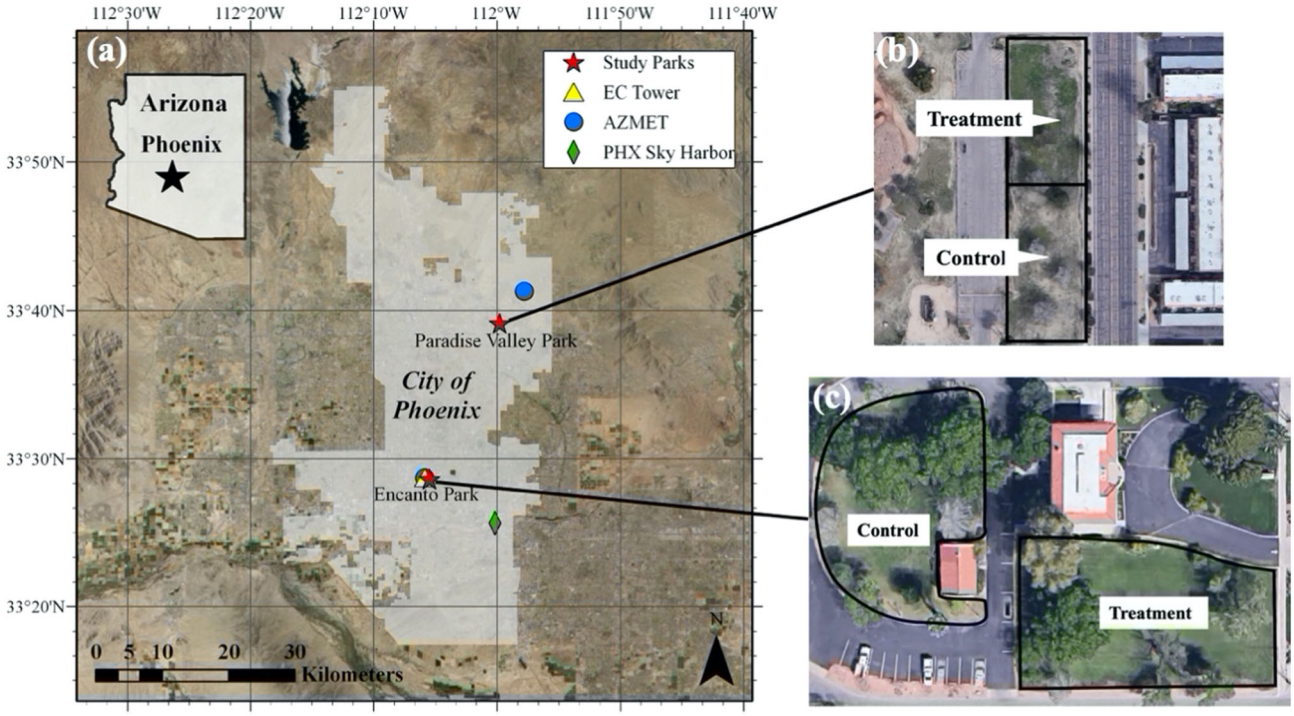

FIGURE 1 (a) Location of study parks, EC Tower, AZMET stations, and Phoenix Sky Harbor Airport. (b) Paradise Valley (PV) park with control and treatment plots. (c) Encanto (EN) park with control and treatment plots

TABLE 1 Study park characteristics, including the sampling duration and dates

Study park	Latitude (dd)	Longitude (dd)	Elevation (m)	Area (km^2)	Soil texture	Irrigation type	Duration (days)	Start and end dates
Paradise Valley Park	33.6522°	−111.9966°	456	0.17	Loam	Sprinkler	615	12/04/18–08/10/20
Encanto Park	33.4771°	−112.0920°	334	0.11	Loam	Flood	679	09/28/18–08/07/20

sites, Figure 1). Over the period 2003 to 2018, the two weather stations had small differences in precipitation (Table 2), which are attributed to an elevation gradient of 122 m over a distance of 27 km (Kindler, 2021). Similarly, modest differences are present in reference evapotranspiration (ET_o) which measures atmospheric demand (1648 and 1513 mm/year at PV and EN, respectively), as estimated by AZMET (https://cals.arizona.edu/AZMET/). The low P and high ET_o at the study parks necessitate the use of irrigation for supporting turf grasses.

3 | METHODS

3.1 | Soil moisture and evapotranspiration measurements

We deployed soil moisture and precipitation sensors at the control and treatment plots in each park during two warm and two cool seasons from 2018 to 2020 (Table 1). Each station included four soil dielectric impedance sensors (HydraProbe, Stevens, Portland, OR), buried at depths of 5, 15, 30 and 50 cm capturing the turf grass root zone depth over 60 cm, and a tipping bucket rain gauge (TE525-L, Texas Electronics, Dallas, TX) installed at 2 m height, connected to a datalogger (CR800, Campbell Scientific, Logan, UT) powered by a solar panel and battery. Siting of each station involved interactions with the Parks and Recreation Department to ensure minimum disturbance of park activities and the replacement of turf grass after installation. Where needed, a fence was placed around a station to protect equipment. Volumetric soil moisture (θ in m^3/m^3) was obtained from continuous voltage readings at 30-min resolution after applying a calibration relation derived for each park (Kindler, 2021). Daily aggregations of θ (averaged) and P (total) were conducted to match the temporal resolution of the soil water balance model. In addition, a depth average of daily θ over the soil profile (0 to 60 cm) was obtained using a weighting scheme (weights of 0.15 at 5 and 15 cm and 0.30 for the 30- and 50-cm sensors), following Templeton et al. (2014). Daily, profile-averaged θ at the control and treatment plots of PV and EN parks were used to test the model. We also tested θ differences between C and T plots using the Wilcoxon signed-rank test at a 5% significance.

For model forcing, we used daily P and ET_o from the two AZMET stations due their long-term records. ET_o was estimated following the procedure outlined by Brown et al. (2001) based on the

TABLE 2 Precipitation characteristics at three locations in Phoenix, organized by month and season (Cool: 1 October to 30 March; Warm: 1 April to 30 September)

		Phoenix Sky Harbor Airport		Desert Ridge AZMET		Phoenix Encanto AZMET	
Season	Month	Average *P* (1950–2018) (mm)	% Annual	Average *P* (2003–2018) (mm)	% Annual	Average *P* (2003–2018) (mm)	% Annual
Cool	Oct.	14.00	7.47%	11.51	5.28%	8.76	4.67%
	Nov.	14.85	7.93%	16.18	7.43%	15.16	8.08%
	Dec.	20.94	11.18%	28.43	13.05%	17.95	9.56%
	Jan.	20.27	10.82%	31.43	14.42%	21.57	11.49%
	Feb.	17.90	9.56%	28.40	13.03%	22.83	12.16%
	Mar.	21.12	11.27%	20.49	9.40%	12.56	6.69%
	Subtotal	109.80	58.23%	136.44	62.62%	98.83	52.64%
Warm	Apr.	6.49	3.46%	7.79	3.58%	5.90	3.14%
	May	3.33	1.78%	3.98	1.83%	3.25	1.73%
	Jun.	2.24	1.20%	0.63	0.29%	3.97	2.11%
	Jul.	22.98	12.27%	24.49	11.24%	23.32	12.42%
	Aug.	25.88	13.82%	29.03	13.32%	37.35	19.90%
	Sep.	17.32	9.25%	15.54	7.13%	15.11	8.05%
	Subtotal	78.24	41.77%	81.46	37.38%	88.90	47.36%
	Total	187.32	100.00%	217.90	100.00%	187.73	100.00%

Penman–Monteith equation applied to well-watered turf grass. The method requires daily net radiation, atmospheric and vapour pressure, wind speed, and air temperature which were estimated at the AZMET stations. Actual evapotranspiration (ET_t) at each park was obtained as $ET_t = K_c ET_o$ and used to verify the soil water balance model. This followed the monthly crop coefficients (K_c) of Brown and Kopec (2014) that include considerations of turf type and quality, with values ranging from 0.60 to 0.89. To corroborate ET_t, we deployed an eddy covariance (EC) tower next to the Phoenix Encanto AZMET station, as documented by Vivoni et al. (2020). Similar EC studies in Phoenix by Chow et al. (2014), Templeton et al. (2018) and Pérez-Ruiz et al. (2020) have illustrated the value of the approach for studying the impact of irrigation. Daily values of evapotranspiration obtained from the EC tower were available over the period 16 March 2019 to 15 July 2020. Due to the shorter record as well as differences in turf grass management at the AZMET station, the EC measurements are only used to corroborate ET_t.

3.2 | Vegetation and irrigation data sets

We monitored turf grass conditions using photographs at control and treatment plots taken at similar viewing angles during monthly intervals (Kindler, 2021). We also processed high spatiotemporal resolution data on the Normalized Difference Vegetation Index (*NDVI*) from Planet Labs, a commercial satellite operator (Planet Team, 2017) to quantify turf grass conditions. The Planet surface reflectance product (3 m, daily resolution, Level 3B Ortho Scene Product) in four spectral bands (Red, Green, Blue and Near Infrared) were obtained from a constellation of >130 active Cubesats deployed in a sun synchronous orbit at the height of 475 km and with an overpass time from 9:30 to 11:30 AM in Phoenix. *NDVI* was obtained as $(Red - NIR)/(Red + NIR)$, where *Red* and *NIR* are the Red and Near Infrared bands. Bias correction was used to adjust *NDVI* to match coincident values from Landsat 8 which have been used often in Phoenix (e.g., Buyantuyev et al., 2007). Available scenes during the study period were then linearly interpolated using the approach of Chen et al. (2004) to produce a smoothened daily time series averaged for selected pixels in the control and treatment plots. We tested differences in daily *NDVI* at the C and T plots in each park using the non-parametric Wilcoxon signed-rank test at 5% significance level.

Irrigation practices varied at the two study parks necessitating a different approach for estimating daily irrigation (I) as a model input (Volo et al., 2014). An automated sprinkler system at PV delivered frequent and small irrigation amounts to the control and treatment plots, while EN was periodically inundated with large watering depths at C and T plots. Both sprinkler and flood irrigation techniques were adjusted during the warm and cool seasons, with monthly irrigation volumes reported by the Parks and Recreation Department. Monthly totals at each park were converted to watering depths using the area of turf grasses under irrigation (Table 1) and subsequently distributed into daily values using the following information: (1) flood irrigation dates, (2) recorded changes in shallow soil moisture and (3) unintended measurement of sprinkler water by rain gauges at the plots. The latter required use of the AZMET stations for *P*. As noted by Volo et al. (2014) and Wang, Vivoni, et al. (2021), obtaining reliable irrigation information is one of the principal challenges for modelling urban areas with differing landscaping designs.

3.3 | Soil water balance model

We applied the soil water balance model of Laio et al. (2001), as modified by Volo et al. (2014) to account for irrigation input and meteorological forcing. The change in relative soil moisture, $s = \theta/n$ (−), averaged over a rooting depth (Z_r) is the result of water fluxes as follows:

$$nZ_r\frac{ds}{dt} = P + I - Q(s) - L(s) - ET(s)\ , \tag{1}$$

where n (−) is porosity and the fluxes are precipitation (P), irrigation (I), runoff (Q), leakage (L) and evapotranspiration (ET, all in mm/day). A numerical approach was applied at the daily step t such that inputs ($P + I$) were added to s from the previous time, resulting in an intermediate s used for determining water losses (Q, L and ET). Q occurred when water inputs resulted in values of $s > 1$ as $Q = nZ_r(1 - s)$. L below the rooting depth Z_r occurred when $s \geq s_{fc}$ as follows:

$$L(s) = K_s\frac{e^{\beta(s-s_{fc})} - 1}{e^{\beta(1-s_{fc})} - 1}\ , \tag{2}$$

where K_s is the saturated hydraulic conductivity (mm/day), s_{fc} is the field capacity of soil (−), $\beta = 2b + 4$ and b is the pore size distribution index (Laio et al., 2001). ET was modelled as a function of s using threshold values of s (all in −) determined by soil and vegetation properties as follows:

$$ET(s) = \begin{cases} 0 & s \leq s_h \\ \dfrac{s - s_h}{s_w - s_h}E_w & s_h < s \leq s_w \\ E_w + \dfrac{s - s_w}{s^* - s_w}(ET_{max} - E_w) & s_w < s \leq s^* \\ ET_{max} & s^* < s \leq 1 \end{cases}, \tag{3}$$

where s_h is the hygroscopic point, s_w is the wilting point, s^* is the stress threshold and E_w is the rate of evaporation below the wilting point (mm/day). We labelled the amount of ET occurring below s_w as E_b (bare soil evaporation), the amount of ET between s_w and s^* as ET_s (stressed evapotranspiration) and the amount of ET taking place between s^* and 1 as ET_u (unstressed evapotranspiration). Daily ET_{max} was obtained as ET_o (mm/day) at the AZMET stations using meteorological variables and the Penman–Monteith equation as follows:

$$ET_o = \frac{0.408\Delta R_n + \gamma\frac{900}{T+273}u(e_s - e_a)}{\Delta + \gamma(1 + 0.34u)}, \tag{4}$$

where R_n is net radiation (MJ/m^2/day), T is air temperature (°C), u is wind speed (m/s), e_s and e_a are the saturated and actual vapour pressures (kPa), and Δ and γ are the slope of the saturation vapour pressure curve and the psychometric constant (both in kPa/°C). Since R_n is not directly measured, the value is obtained from incoming solar radiation as indicated by Brown (2005).

Plant water stress (ζ) was calculated in relation to the stress threshold (s^*), at which stomatal closure is induced ($\zeta = 0$), and the wilting point (s_w) when transpiration ceases ($\zeta = 1$):

$$\zeta(s) = \left(\frac{s^* - s}{s^* - s_w}\right)^q, \tag{5}$$

where q represents the nonlinearity of the relation between soil moisture deficit and plant health (Porporato et al., 2001). Following Volo et al. (2014), we assumed $q = 3$. The average dynamic water stress (Θ) over a season (T_{seas}) was obtained as follows (Rodríguez-Iturbe & Porporato, 2004):

$$\Theta = \begin{cases} \left(\dfrac{\overline{\zeta'}\overline{T}_{s*}}{kT_{seas}}\right)^{1/\sqrt{\overline{n}_{s*}}} & \text{if } \overline{\zeta'}\overline{T}_{s*} < kT_{seas}, \\ 1 & \text{otherwise} \end{cases}. \tag{6}$$

Here, $\overline{n}_{s*}$ is the average number of periods in a growing season with $s < s^*$, and $\overline{T}_{s*}$ and $\overline{\zeta'}$ are the average duration and intensity of these periods. Θ was evaluated for both cool and warm seasons, each with T_{seas} of 180 days. k represents the ability of a plant to withstand prolonged water stress without permanent damage and was assumed $k = 0.5$ based on Porporato et al. (2001). Both daily values of ζ and seasonal values of Θ range from 0 (*no stress*) to 1 (*maximum stress*).

3.4 | Model parameterization, calibration and validation

To model s at the control and treatment plots of each study park, estimates of daily P, ET_o and I were provided as model forcings. For model calibration and validation purposes, the profile-averaged volumetric soil moisture (θ) data over the root zone $Z_r = 60$ cm were converted to s using specific values of porosity at each park: (1) at PV, $n = 0.43$ based on soil laboratory analyses, and (2) at EN, $n = 0.66$ based on the maximum observed θ during flood irrigation (Kindler, 2021). Similarly, simulated ET was compared to daily ET_t estimates from the AZMET stations. Comparisons of simulated and observed s and ET were carried out visually as daily time series and frequency distributions as well as through the use of goodness of fit measures, root mean squared error (*RMSE*), correlation coefficient (*CC*) and bias ratio (*B*), with the latter defined as the ratio of the average of the simulated values divided by the average of the observed values. Model calibration was conducted at the C plots for a full year (4 November 2018 to 3 November 2019 at PV; 28 September 2018 to 30 September 2019 at EN) to capture one cool season and one warm season. Initial values of s for the calibration period were obtained from the observed records on the first day. The remainder of the periods (4 November 2019 to 10 August 2020 at PV; 1 October 2019 to 7 August 2020) were reserved for model validation at the control plots (e.g., one cool

and one warm season). Simulations at the T plots were performed with the calibrated parameters to test the model transferability under the presence of the compost treatment. We postulated that if parameters were transferable through visual and statistical comparisons of simulated and observed s at T plots, then the soil water balance model worked equally well at both plot types and the effect of compost on simulated s was limited.

Following Volo et al. (2014), we applied the Shuffled Complex Evolution algorithm of Duan et al. (1993) to calibrate the soil and vegetation parameters at the control plots (e.g., s_h, s_w, s^*, s_{fc}, b, K_s and E_w). n and Z_r were fixed based on soil properties and the rooting depth for bermudagrass (Fuentealba et al., 2015) which matched well with the sampling depth interval of θ. The automated method searched for globally optimal parameter values in a multidimensional space through clustering, shuffled complexes and competitive evolution strategies. We applied the minimization of *RMSE* between observed and simulated s over the calibration period at each control plot as the objective function. Up to 100 independent calibrations were performed for each C plot, with each calibration consisting of 10,000 model runs. The initial parameter bounds were chosen based on relevant literature values (Laio et al., 2001; Manfreda et al., 2010; Porporato et al., 2003; Vico & Porporato, 2010; Volo et al., 2014) and adjusted to avoid retrieving a parameter value equal to a limit of its range or overlapping with another parameter range. Since convergence was achieved during the optimization, we obtained averages of each parameter across the calibration runs (Table 3) and used these in the subsequent modelling activities. Model validation at the C plots utilized the s at the end of the calibration period as an initial state, while the validation at the T plots relied on the observed records of s for the initial day.

3.5 | Numerical simulations and scenarios

To explore a wider range of climatic conditions, we conducted long-term simulations at the C plots using meteorological forcings from AZMET stations (2003–2018, 15 water years, 1 October to 30 September). This period corresponds to the availability of ET_o from the approach of Brown et al. (2001). For a subset of analyses, we selected the driest (2017–2018), an average (2012–2013) and the wettest (2004–2005) years with respect to mean annual precipitation (Table 4). Due to limited irrigation data for the 15-year period, we repeated the daily irrigation records from 2018 to 2019, such that interannual variations in forcing were driven only by changes in P and ET_o. The 15-year periods at the study parks were then used to conduct two sets of irrigation scenarios: (1) variation of annual irrigation totals using the temporal distribution of the first cool and warm seasons and (2) variation of the irrigation depth or frequency corresponding to cases of interest to the Parks and Recreation Department as identified through stakeholder meetings. While more complex irrigation scenarios are possible (e.g., Vico & Porporato, 2011a, 2011b; Volo et al., 2015), we were guided by practitioner feedback on operationally feasible approaches. Four cases were tested: (1) the current schedule and magnitude of events, (2) an 18% reduction in irrigation magnitude, (3) a reduction in irrigation by changing the warm season frequency and (4) a 30% reduction in

TABLE 3 Calibrated model parameters at the study parks with minimum, average, and maximum values obtained from the optimization routine

			Paradise Valley Park			Encanto Park		
Parameter	Units	Symbol	Min.	Average	Max.	Min.	Average	Max.
Hygroscopic point	(−)	s_h	0.04	0.10	0.16	0.10	0.10	0.10
Wilting point	(−)	s_w	0.20	0.20	0.20	0.66	0.67	0.68
Stress threshold	(−)	s^*	0.42	0.42	0.42	0.71	0.73	0.73
Field capacity	(−)	s_{fc}	0.43	0.61	0.82	0.74	0.74	0.74
Pore size distribution index	(−)	b	5.80	7.48	8.98	10.85	10.85	11.05
Saturated hydraulic conductivity	(mm/day)	K_s	171.68	255.18	320.77	289.42	289.42	295.54
Wilting point evaporation	(mm/day)	E_w	0.17	0.17	0.17	1.50	1.50	1.50

TABLE 4 Seasonal and annual precipitation for Dry, Average and Wet years at AZMET stations

	Desert Ridge AZMET			Phoenix Encanto AZMET		
Year	Cool season (mm)	Warm season (mm)	Annual total (mm)	Cool season (mm)	Warm season (mm)	Annual total (mm)
Dry: 2017–2018	77.96	36.82	114.78	52.31	59.70	112.01
Average: 2012–2013	72.90	143.48	216.38	67.55	90.66	158.21
Wet: 2004–2005	104.15	291.07	395.22	106.43	233.41	339.84

irrigation magnitude. Irrigation reductions were based on a water savings potential that could offset the additional cost of compost treatments, as compared to traditional fertilizers. For the scenarios, we quantified monthly soil moisture dynamics (s), water balance components (P, I, ET, L and Q), and the dynamic water stress (Θ) for cool and warm seasons.

4 | RESULTS

4.1 | Soil moisture, evapotranspiration and vegetation observations

Figure 2 illustrates the daily variations in P, θ and ET_o during the study periods at the control and treatment plots at PV and EN. Note that most of the precipitation was concentrated during the cool seasons (95% of annual total), which were anomalously wet (187% of 2003–2018 values), whereas the warm seasons exhibited lower-than-average P (14% of 2003–2018). While profile-averaged θ reacted to storms in the cool seasons, the primary response was to irrigation events in each park. Based on water use records, irrigation accounted for 81% and 85% of water input ($P + I$) at the PV and EN study parks, respectively. At PV, frequent warm season sprinkler use resulted in small, daily increases in θ, whereas flood irrigation at EN led to larger pulses in θ spaced about 2 weeks apart. Reductions in θ after each irrigation were driven by high values of ET_o during the warm season (average of 6.2 mm/day across both parks), while cool season ET_o was more modest (2.3 mm/day) and resulted in slower recessions after each irrigation (Kindler, 2021). Clearly, soil moisture varied substantially between the two parks. For instance, the range of θ at PV was between 0.09 and 0.22 m^3/m^3 for the control plot (average and standard deviation of 0.14 ± 0.02 m^3/m^3), while the C plot at EN exhibited higher values of θ from 0.36 to 0.61 m^3/m^3, resulting in 0.48 ± 0.05 m^3/m^3. Furthermore, the warm seasons had similar values of θ (0.14 ± 0.02 and 0.48 ± 0.05 m^3/m^3 at PV and EN) as compared to the cool seasons (0.14 ± 0.02 and 0.48 ± 0.04 m^3/m^3 at PV and EN) at the C plots, as a compensating effect occurred between the higher irrigation input in the warm seasons and the higher precipitation during the cool seasons.

We compared the daily ET_o at the Phoenix Encanto AZMET station to the co-located EC measurements to ensure the model forcing was sound (Figure 3). As noted by Vivoni et al. (2020), the seasonality in actual ET measured by the EC system was captured well by ET_o, with similar average seasonal values (e.g., 5.7 and 6.2 mm/day for warm, and 2.1 and 2.2 mm/day for cool seasons). As expected, monthly ET_o was typically larger than actual ET. For some days (33% of period), ET exhibited higher values than ET_o due to: (1) the effects of advected energy from surrounding urban areas during the warm

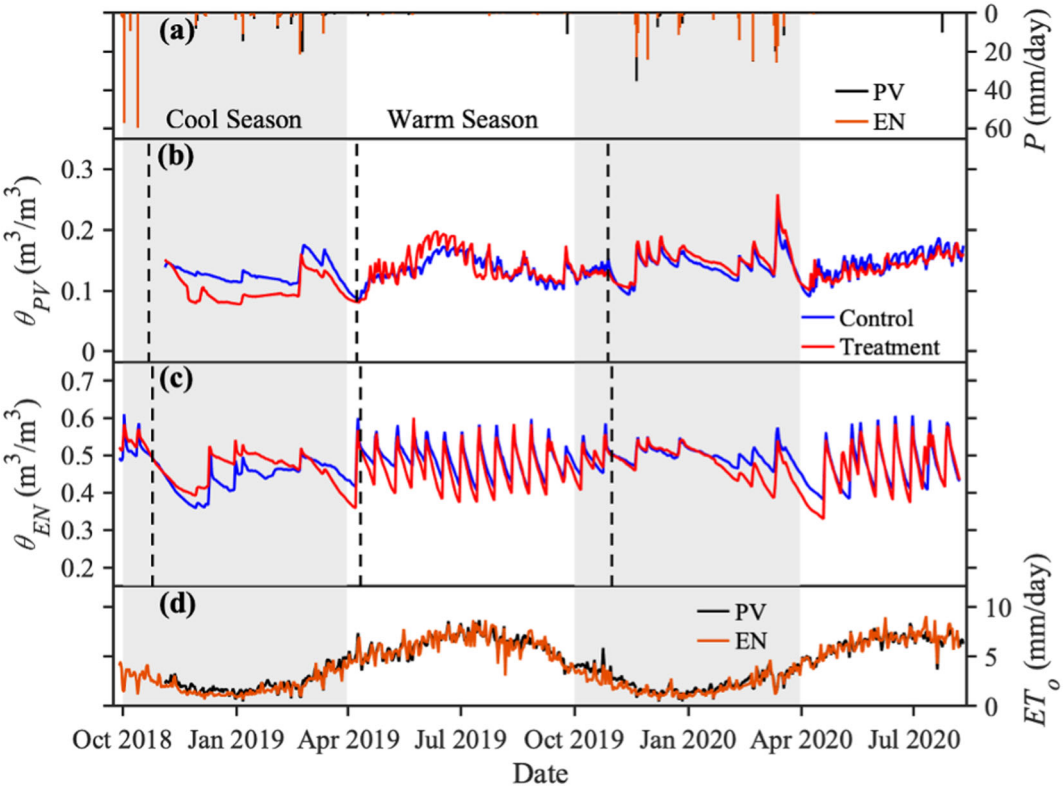

FIGURE 2 Daily hydrological observations at Paradise Valley (PV) and Encanto (EN) parks, including (a) Precipitation (P), (b, c) Volumetric soil moisture averaged over the soil profile at PV and EN (θ_{PV} and θ_{EN}), and (d) reference evapotranspiration (ET_o) from AZMET stations. Vertical dashed lines indicate the compost application dates at each park. The shaded and nonshaded regions depict the cool and warm season, respectively, over the study period

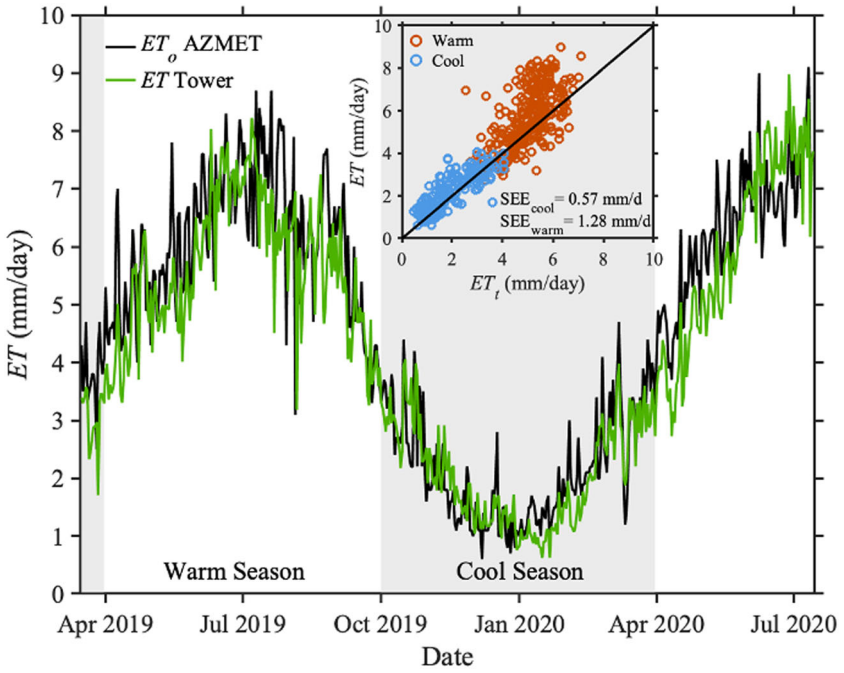

FIGURE 3 Comparison of daily reference evapotranspiration (ET_o) from AZMET station and actual evapotranspiration (ET) measured by the eddy covariance tower at Encanto Golf Course during the overlapping period. The inset shows a scatterplot comparison of ET and $ET_t = K_c ET_o$ for warm and cool seasons days, with associated values of the standard error of estimates (SEE)

season on the local energy balance (see Vivoni et al., 2020) and (2) inaccuracies in the estimation of R_n in the Penman–Monteith approach of Brown et al. (2001). This is further illustrated in the comparison of ET and ET_t (Figure 3, inset). During the cool season, ET_t slightly underestimated ET (low standard error of estimates, $SEE = 0.57$ mm/day, measuring average distance to 1:1 line), whereas a higher underestimation of ET by the AZMET methodology was present during the warm season ($SEE = 1.28$ mm/day). Despite these small inaccuracies, the seasonal variations in evapotranspiration in the turf grass site were appropriately represented. For instance, the difference between the warm and cool season average values of ET_t (3.7 mm/day) was similar to the seasonal difference in ET (3.7 mm/day). This indicated that seasonality in the soil water balance model can be captured through changes in ET_o. A similar approach was adopted by Caylor et al. (2005) and Volo et al. (2014).

Figure 4 displays the temporal variation in turf grass greenness as captured by *NDVI* values averaged over C and T plots in each study park. As expected, warm seasons exhibited a higher daily average *NDVI* (0.57 and 0.47 at PV and EN, respectively) than the cool seasons (0.49 and 0.39). Absolute differences between the study parks are attributed to variations among Cubesat reflectance values. As such, the relative values of *NDVI* between the C and T plots within each park are emphasized. Note that abrupt transitions in *NDVI* occurred between seasons in response to changes in irrigation and turf grass phenology. This is shown in Figure 4 through a spatial comparison of 2 days (15 July 2019 and 15 December 2019) representing warm and cool seasons. Note that the outlines of the irrigated areas in each park are clearly visible and that contrasts between the turf grass areas and the surrounding roads and buildings are enhanced in the warm season. As observed for the profile-averaged θ (Figure 2), *NDVI* within the control and treatment plots have visually similar behaviour, with some exceptions when irrigation might have varied or the impact of precipitation events differentially influenced the turf grass areas.

4.2 | Comparisons of control and treatment observations

We compared soil moisture and vegetation conditions at control and treatment plots to determine if the green waste compost applications yielded a measurable impact. Figure 5 presents scatterplots of daily, profile-averaged θ for cool and warm seasons between C and T plots at the two study parks. No consistent bias is found in the comparison, with some periods having larger θ alternatively at the control and treatment plots. In addition, low values were found for *SEE*. The Wilcoxon signed-rank test showed significant differences for the total period at EN but not at PV, with several seasons exhibiting values of $p < 0.05$ despite the small absolute differences (Table 5). These small differences are attributed to (1) the effects of initial sensor installation for the cool season of 2018–2019 (i.e., soil settling around sensors) and (2) small variations in irrigation, in particular for the warm season of 2020 at PV and for the warm season of 2019 at EN. Similarities between control and treatment plots were also found in *NDVI* (Table 5), with no consistently greater values at the T plots as would be anticipated if compost treatments enhanced turf grass health. While certain seasons had statistically significant differences, these were explained by variations in θ linked to the causes described above. Where discrepancies in the relative values of θ and *NDVI* were present between control and treatment plots (i.e., cool season of 2018–2019), these were due to the initial installation leading to non-representative soil moisture as compared to the vegetation conditions captured within the plot through *NDVI*. Overall, the comparisons of C

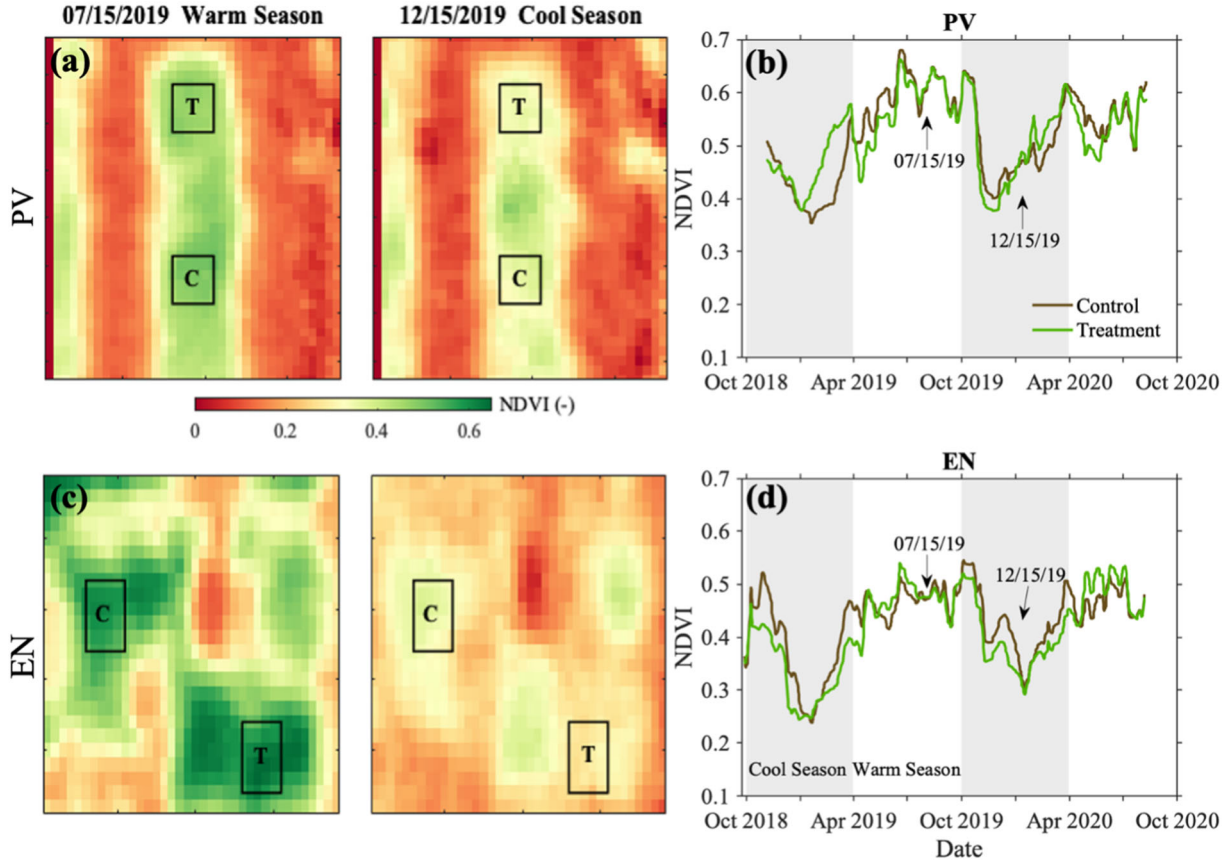

FIGURE 4 Vegetation greenness obtained from *NDVI* at the PV and EN study parks shown as: (a, c) spatial maps for selected dates and (b, d) smoothed daily time series

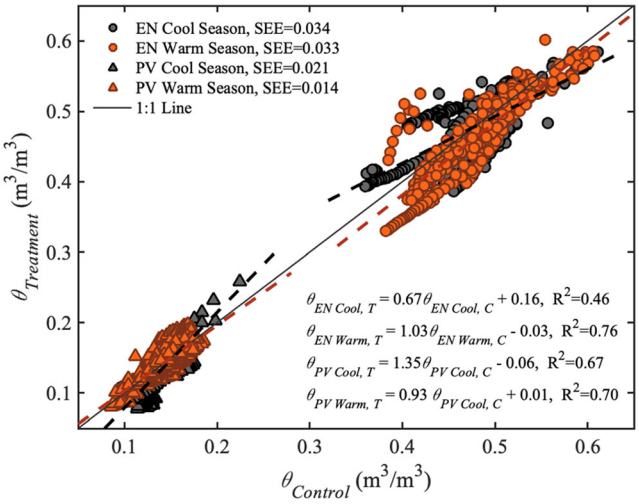

FIGURE 5 Comparison of daily, profile-averaged volumetric soil moisture between control and treatment plots for PV and EN parks during the cool and warm seasons in the study period, with associated values of the standard error of estimates (*SEE*) in m^3/m^3. Linear regression equations are shown for each park and season, along with associated R^2 values

and T plots suggest that the green waste compost applied twice per year did not have a consistent impact on soil moisture dynamics or vegetation greenness.

4.3 | Comparison of observed and simulated soil moisture and evapotranspiration

Figure 6 compares the observed and simulated *s* based on the calibrated parameters reported in Table 3 for C and T plots at both study parks. Calibration periods are shown in grey shading. Validation periods used the same parameter sets, except for the specification of the initial value of *s*. Daily forcing included the observed *P* and estimates of ET_o and *I*. At PV, small and frequent irrigation pulses were applied (e.g., <10 mm/day, daily application in the warm season), which led to a total *I* of 1325 mm over the study period. In contrast, EN was managed with a few large pulses (e.g., >80 mm/day, once every 2 weeks in the warm season), resulting in an estimated *I* of 2400 mm over the entire period for the C plot with a higher value at the T plot due to two additional irrigation events (Table 6). Irrigation pulses at PV were smaller than *P* events, whereas the opposite was the case at EN. Furthermore, while most *I* was applied during the warm seasons, the Parks and Recreation Department carried out a few irrigation events during the cool seasons to sustain large, deeply rooted trees surrounding the turf grass areas.

Model simulations performed well with respect to the observed *s* during calibration and validation periods at the C plots and for the validation period at the T plots in both parks. For instance, the model distinguished between the slow recession of *s* during cool seasons

TABLE 5 Statistical comparison of *NDVI* and profile-averaged θ (average values and standard deviation [Std]) for control (C) and treatment (T) plots at the two study parks during entire study period (Table 1) and two warm seasons (1 April to 30 September)

Study park	Variable and period	C average	C Std	T average	T Std	*p* value
PV	*NDVI* (–)					
	Total period	0.53	0.08	0.52	0.07	0.15
	Cool season 2018–2019	0.43	0.06	**0.47**	0.06	7.3×10^{-6}*
	Warm season 2019	0.59	0.05	0.57	0.06	4.7×10^{-5}*
	Cool season 2019–2020	0.51	0.07	0.51	0.08	0.63
	Warm season 2020	0.56	0.03	0.54	0.04	1.9×10^{-4}*
	Profile-average θ (m^3/m^3)					
	Total period	0.14	0.02	0.13	0.03	0.54
	Cool season 2018–2019	0.13	0.02	0.10	0.02	2.8×10^{-21}*
	Warm season 2019	0.13	0.02	0.14	0.03	0.28
	Cool season 2019–2020	0.14	0.02	**0.15**	0.02	1.5×10^{-2}*
	Warm season 2020	0.14	0.02	0.14	0.02	0.02*
EN	*NDVI* (–)					
	Total period	0.44	0.07	0.43	0.08	0.04*
	Cool season 2018–2019	0.38	0.09	0.34	0.07	3.2×10^{-5}*
	Warm season 2019	0.47	0.03	0.47	0.04	0.55
	Cool season 2019–2020	0.43	0.07	0.40	0.06	1.5×10^{-5}*
	Warm season 2020	0.47	0.03	**0.49**	0.04	3.3×10^{-9}*
	Profile-average θ (m^3/m^3)					
	Total period	0.48	0.05	0.47	0.05	7.0×10^{-3}*
	Cool season 2018–2019	0.45	0.05	**0.47**	0.05	1.3×10^{-5}*
	Warm season 2019	0.49	0.04	0.47	0.05	2.3×10^{-5}*
	Cool season 2019–2020	0.50	0.02	0.48	0.04	3.4×10^{-4}*
	Warm season 2020	0.47	0.06	0.46	0.07	0.78

Note: Statistically significant differences from the Wilcoxon signed-rank test ($p < 0.05$) are shown with asterisks. Bold values indicate when T plots had higher values than C plots that were statistically significant.

and the more abrupt decreases after warm season irrigation. The soil moisture response to irrigation and the range of observed *s* values were also captured well. Notably, the model reproduced the behaviour of both sprinkler and flood irrigation types through the applied model forcings and parameter values. Table 6 presents statistical comparisons of the observed and simulated *s* based on the *RMSE*, *CC* and *B* metrics. At PV, the validation performance was nearly equal to that of the calibration at the C plot, while a lower model skill was noted for the validation at the T plot. At EN, the model performance was slightly lower for the validation period at the control plot, but the validation at the treatment plot was comparable to the control calibration. As noted in the statistical comparison of θ between C and T plots, there were only a few differing behaviours in model performance across the plot types at both parks. For instance, simulations did not capture well: (1) the initial cool season at the PV treatment plot when sensor installation effects were notable and (2) periods of time when the irrigation input varied between C and T plots.

To complement the model evaluation, Figure 7 compares the frequency distributions of *s* and *ET* for calibration and validation periods corresponding to each study park. Daily simulated (sim) values of *s* and *ET* resulted from the soil water balance model, whereas daily observed (obs) values were obtained from θ and ET_t. For reference, model parameter values (s_w, s^* and E_w) are shown. Simulated frequency distributions corresponded well with the observed *s* values over the full range of conditions, in particular for the calibration periods. As noted earlier, model skill was lower for the treatment validation at PV and the control validation at EN. Nevertheless, the range of values of *s* and the peak frequencies at a particular *s* were generally captured well in the simulations. Values of *s* at PV were typically within the bounds of s_w and s^*, indicating that simulated *ET* was under a stressed condition (ET_s, Laio et al., 2001), whereas values of *s* at EN were often lower than s_w or higher than s^*, such that simulated *ET* fluctuated between E_b and ET_u. Indeed, ET_t showed a bimodal frequency distribution at both study parks. This behaviour was the result of seasonal variations of ET_o, with low ET_t during cool seasons and high ET_t during warm seasons. To some extent, simulations captured the bimodality of ET_t, for instance during the validation period at the PV control plot, but also had difficulty in matching high ET_t. These discrepancies were attributed to the simplified use of a monthly K_c to determine ET_t as opposed to the daily variation of ET_{sim} resulting from

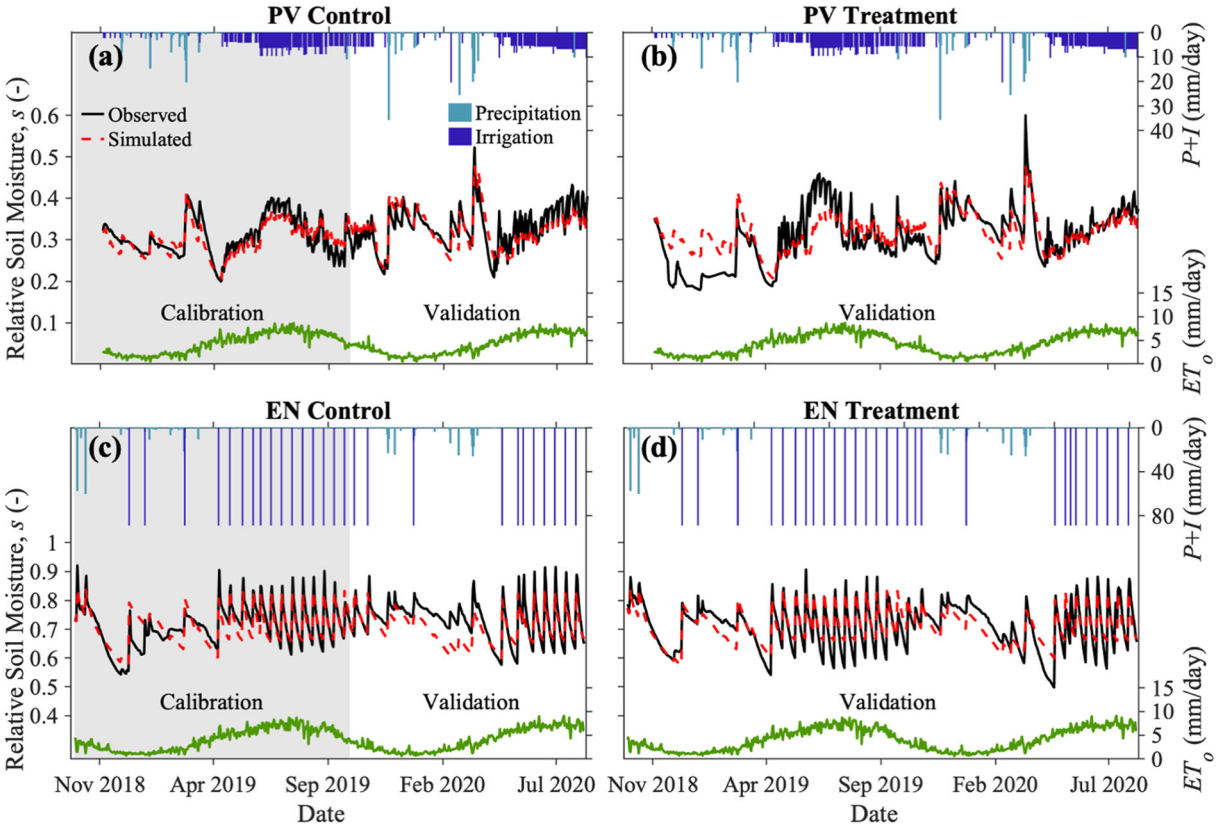

FIGURE 6 Comparison of observed and simulated relative soil moisture (*s*) over the calibration (shaded) and validation (non-shaded) periods: (a, b) PV for control and treatment plots, and (c, d) EN for control and treatment plots. Note that treatment plots were used as model validation. Daily precipitation and irrigation inputs as well as reference evapotranspiration are shown

TABLE 6 Model performance metrics (root mean squared error, *RMSE*, correlation coefficient, *CC*, and bias ratio, *B*) of relative soil moisture (*s*) at control and treatment plots at the study parks for calibration and validation periods

				Relative soil moisture (*s*) metric		
Study park	**Period and plot**	**Precipitation (mm)**	**Irrigation (mm)**	***RMSE*** **(m^3/m^3)**	***CC*** **(–)**	***B*** **(–)**
PV	Calibration					
	Control[a]	127.50	765.57	0.025	0.83	0.99
	Validation					
	Control[b]	189.95	559.86	0.026	0.83	0.98
	Treatment[c]	317.45	1325.43	0.046	0.74	1.03
EN	Calibration					
	Control[d]	226.24	1422.40	0.042	0.80	1.00
	Validation					
	Control[e]	211.55	977.90	0.053	0.73	0.96
	Treatment[f]	437.79	2578.10	0.043	0.83	1.00

[a]4 Nov. 2018 to 3 Nov. 2019.
[b]4 Nov. 2019 to 10 Aug. 2020.
[c]4 Nov. 2018 to 10 Aug. 2020.
[d]28 Sep. 2018 to 30 Sep. 2019.
[e]1 Oct. 2019 to 7 Aug. 2020.
[f]28 Sep. 2018 to 7 Aug. 2020.

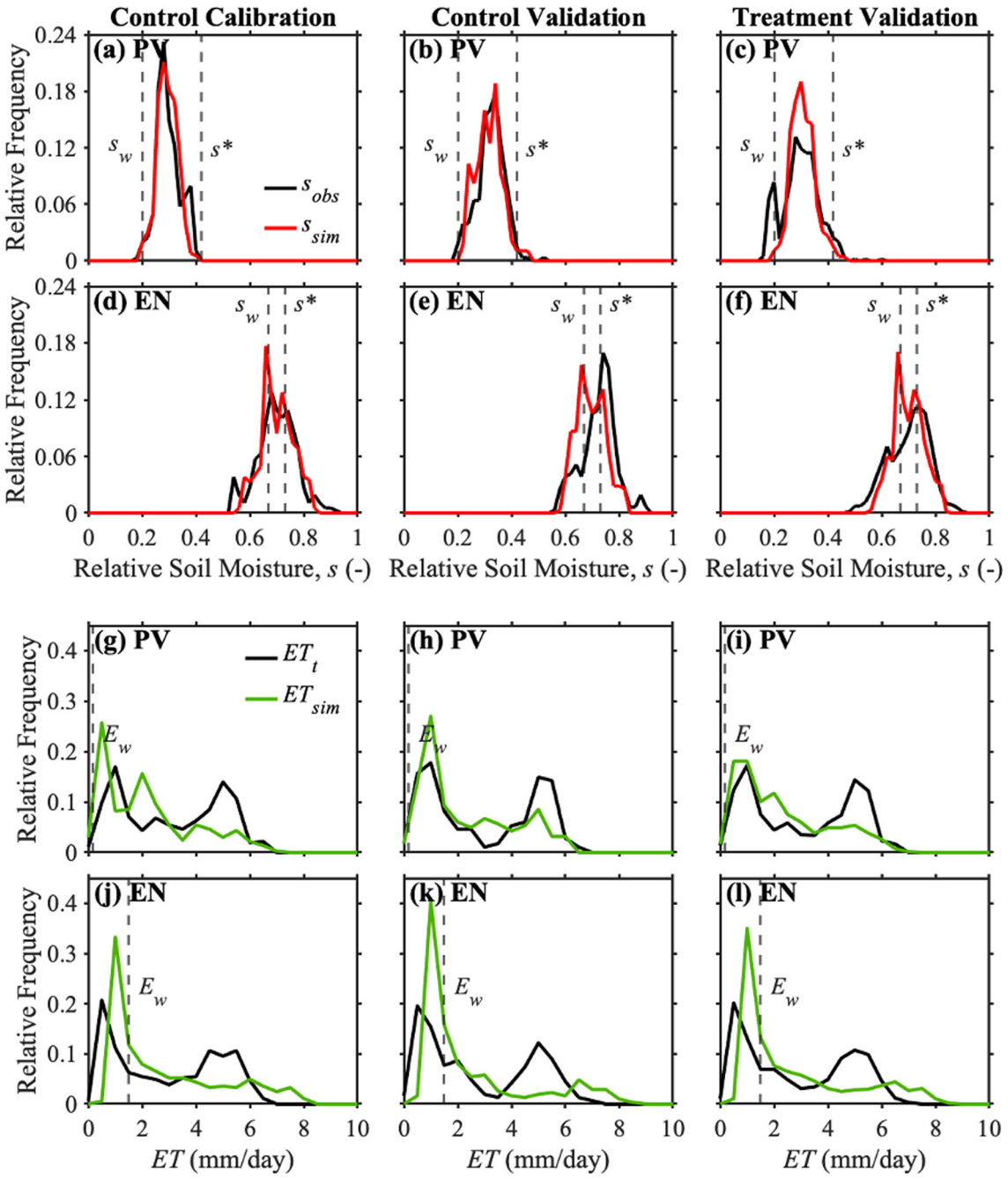

FIGURE 7 Comparison of daily observed (obs) and simulated (sim) hydrologic variables: (a–f) frequency distribution of relative soil moisture (s), and (g–m) frequency distribution of evapotranspiration (ET) for calibration and validation periods at the control plots and for the treatment plot validation. Vertical lines indicate model parameters (s_w, s^* and E_w). Observed ET is denoted by $ET_t = K_c ET_o$ from the corresponding AZMET station

precipitation and irrigation events. At EN, warm season values of ET_{sim} from 6 to 8 mm/day were more consistent with EC data than ET_t.

4.4 | Effect of irrigation amount in long-term scenarios

Given the confidence built on the simulations, we present a set of long-term modelling runs for the C plots of each study park in Figure 8. Monthly s and water balance components (P, I, ET and L) are shown after averaging over the 15-year periods using the AZMET forcing. Q is omitted due to negligible values for the sprinkler and flood irrigation amounts during 2018 to 2019. As expected, precipitation seasonality was similar at the two parks, while I was of higher magnitude (Table 6) and for a longer duration at EN (i.e., flooding applied in all months except January, March and November). The contrast in irrigation type led to variations in the seasonal distributions in s at EN (s from 0.63 to 0.74) as compared to PV (s from 0.25 to 0.37).

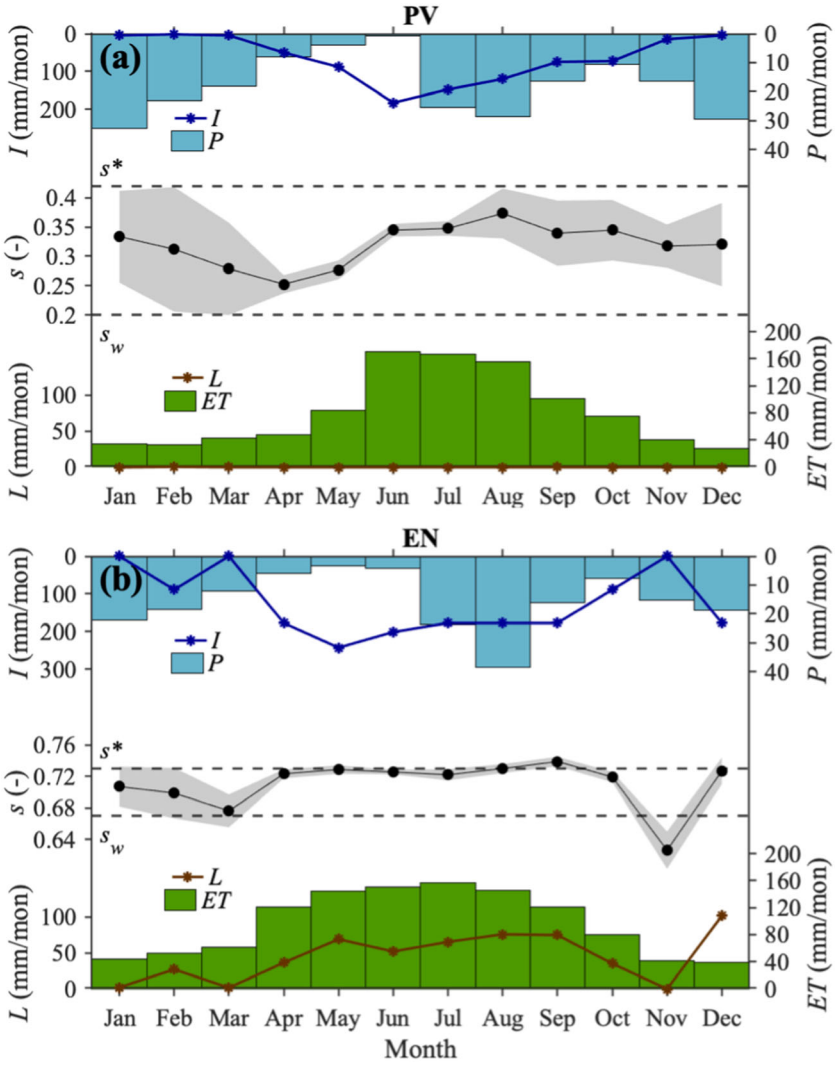

FIGURE 8 Monthly variation of simulated water balance components over 15-year period at: (a) PV and (b) EN parks. Average values shown for precipitation (*P*), irrigation (*I*), evapotranspiration (*ET*), leakage (*L*) and relative soil moisture (*s*). Shaded envelops for *s* depict ±1 monthly standard deviation. Horizontal dashed lines represent calibrated model parameters s^* and s_w

In addition, interannual variations in *s*, denoted by ±1 monthly standard deviation, indicated that soil moisture conditions at EN were less dependent on year-to-year precipitation differences. A major difference in leakage (*L*) beyond the 60 cm root zone was present in the two study parks. While PV had no *L* for the sprinkler irrigation amounts applied, EN exhibited values of *L* ranging from 0 to 101 mm/month. At EN, leakage was present during all months with *I* and showed a maximum value in December as irrigation was applied when ET_o was low. Interestingly, the seasonality of *ET* varied substantially between the study parks. Flood irrigation at EN led to a sustained *ET* (average of 140 mm/month) during the entire warm season, whereas sprinkler irrigation resulted in a shorter period of high *ET* values (average of 164 mm/month between June and August).

Figure 9 compares the sprinkler and flood irrigation practices in terms of their impact on the dynamic water stress, Θ, calculated for the 15 separate cool and warm seasons. The water input ($P+I$) for each season was only sensitive to the interannual variability of *P*, such that linear regressions between Θ and $P+I$ (dashed lines) indicated the role of precipitation. Cool seasons showed a dynamic water stress that was influenced substantially more by *P* than warm seasons, with a more notable effect at PV. Higher values of *I* typically buffered the

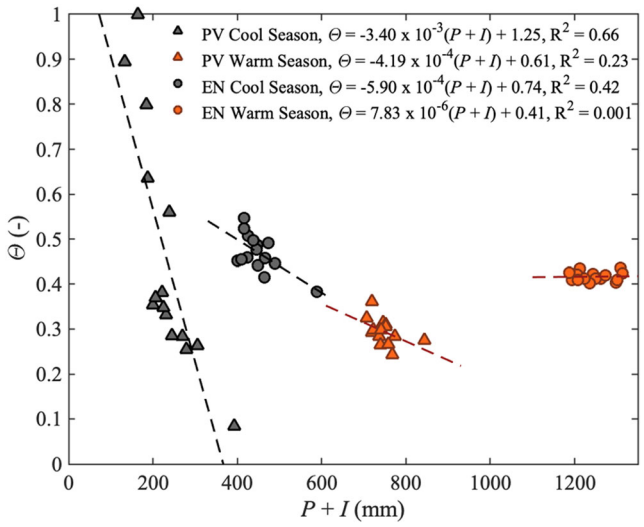

FIGURE 9 Seasonal dynamic water stress (Θ) as a function of total water input ($P+I$) over 15-year period (2003–2018) at the control plots of each study park. Dashed lines represent linear regressions obtained for each park and season with associated R^2 values

effects of interannual precipitation variations, leading to nearly no sensitivity of P in the warm season at EN where I was estimated as 193 mm/month. Furthermore, irrigated conditions led to relatively low values of Θ (from 0.24 to 0.44) as compared to unirrigated arid systems (Porporato et al., 2001). Values of $\Theta > 0.55$ occurred only during cool seasons with below-average P and mostly at PV where sprinkler irrigation applied in small and infrequent pulses could not sustain turf grasses well.

In Figure 10, we show the sensitivity of long-term averaged Θ to the total annual I, which was varied in increments of 13 mm/year using the 2018–2019 distribution. These scenarios are compared to the calibration cases (dashed lines) and scenarios with a reduction of 18% in annual I (solid lines). The sensitivity of Θ is also shown for the Dry, Average and Wet years (Table 4) that depict the interannual variability in P. Θ decreased from values near 1 for the case with no irrigation to values approaching 0.1 at PV and 0.4 at EN. The decrease in Θ was not monotonic since water balance components (E_b, ET_s, ET_u, L and Q) exhibited thresholds at specific values of annual I. For instance, dynamic water stress increased at EN for $I > 1400$ mm/year due to the generation of Q, which reduced available s and increased Θ. At the values of I for the calibration period, the cool season has higher Θ than the warm season (0.46 and 0.30 at PV, and 0.47 and 0.42 at EN for cool and warm seasons). As I was reduced, a cross-over point was identified when the turf grasses during the warm season became more stressed, at 467 and 240 mm/year for PV and EN. As expected, the Dry year had a higher Θ, while the Wet year showed a lower Θ. Higher sensitivity of Θ to the annual P was noted at PV as compared to EN. Precipitation also influenced the cross-over point such that Θ had different sensitivities to I across years. At the calibrated I value, the water balance was partitioned into ET_s and ET_u at PV, and into ET_s, ET_u, and L at EN, with a smaller amount of E_b. As explored in more detail next, a reduction of 18% of annual I did not appreciably change the water balance components or the dynamic water stress in either park as compared to the current irrigation. Two exceptions were noted in that the 18% reduction led to (1) an increased warm season Θ by 0.12 at PV and (2) a reduced L by 261 mm/year at EN.

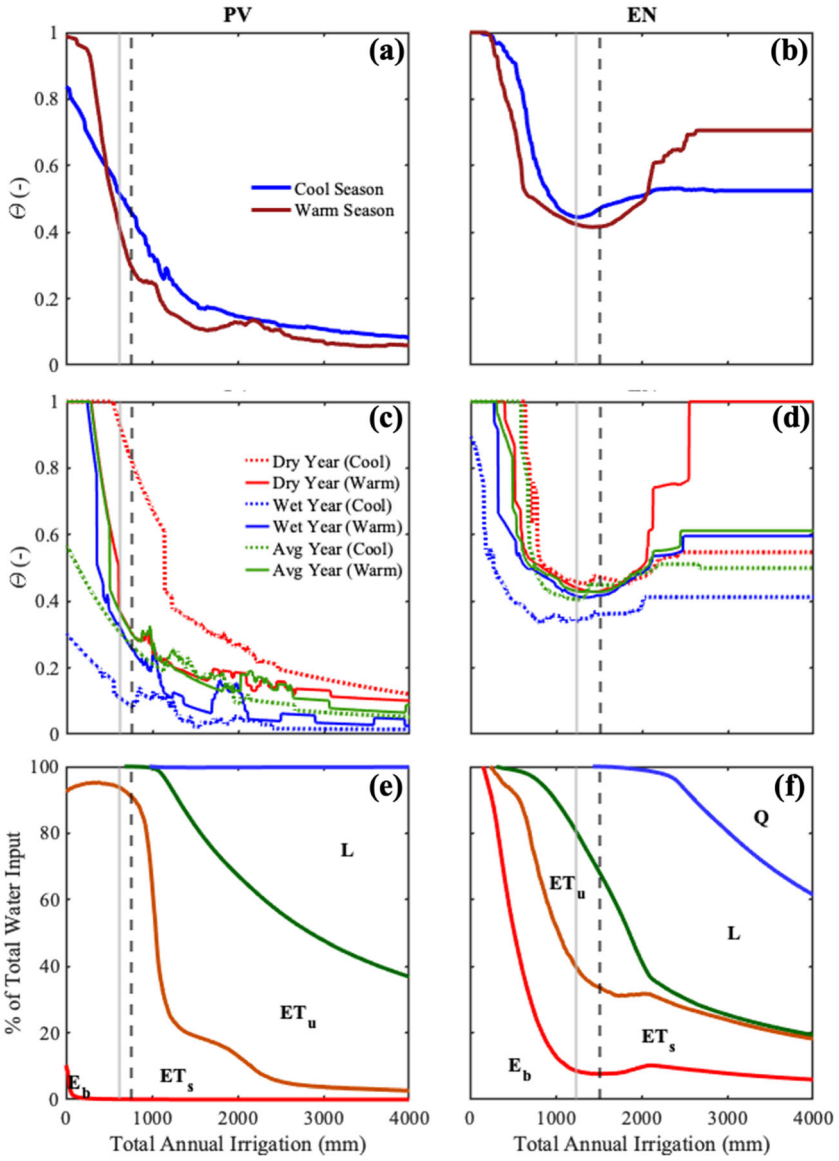

FIGURE 10 Dynamic water stress and water balance components as a function of annual irrigation for PV and EN study parks. (a, b) Seasonal values for warm and cool season averaged over 15-year periods. (c, d) seasonal Θ for Dry, Average and Wet years (Table 4). (e, f) annual average components over 15-year periods. Grey vertical dashed lines represent the calibrated irrigation input. Grey vertical solid lines represent target water savings amount (18%)

4.5 | Stakeholder-driven water savings scenarios

As part of the stakeholder meetings, we conducted scenarios that explored the potential for water conservation through changes in irrigation. The four scenarios (1 to 4) are described in Table 7, including the irrigation amount, the percentage of water conserved, and average Θ and L for cool and warm seasons during the 15-year simulations. An 18% reduction in annual I through a change in magnitude (Scenario 2) led to a small increase in Θ for the warm season at PV and no impact at EN, whereas a large reduction of L of 261 mm/year was achieved at EN. Reaching a similar water savings target (19% at PV and 15% at EN) using a change in irrigation frequency (Scenario 3) increased warm season Θ, relative to Scenario 2, and had a smaller impact on L (65 mm/year reduction). This suggests that changes in irrigation magnitude were more effective. As a result, Scenario 4 tested if a larger 30% reduction in magnitude could be supported, resulting in a slightly higher impact on warm and cool season Θ at PV and no appreciable change at EN, while greatly reducing L at EN (387 mm/year). Results were presented to stakeholders using Figure 11 to show the water balance components for the scenarios. Through these graphs, we communicated that irrigation reductions were possible without adverse effects on turf grasses and with the benefit of reducing ET_u at PV and reducing L at EN. We noted that less sprinkler irrigation at PV led to a lower unstressed evapotranspiration that likely would reduce lawn maintenance costs, while less flood irrigation at EN reduced the water lost below the turf grass root zone.

5 | DISCUSSION

5.1 | Compost effect on soil and vegetation conditions

Differences in profile-averaged θ and *NDVI* between the control and treatment plots were small and inconsistent (Table 5). Significant variations were attributable to the effects of initial installation or minor disparities in irrigation input. Furthermore, the soil water balance model calibrated at the control plots performed equally well for the compost treatment plots (Figure 6). This parameter transferability indicates that no additional biophysical processes were necessary for simulating soil moisture under a compost treatment. In contrast, Whitney et al. (2017) found that adding a physical representation of a biological crust layer to the soil water balance model was required to properly reproduce soil moisture observations. These multiple lines of evidence indicate that green waste compost applications in these urban parks does not conserve water in such a way as to offset its higher costs as compared to traditional fertilizers. Furthermore, measurable improvements on vegetation conditions were also not identified. These findings are conditioned on the use of a thin layer of compost incorporated into a turf grass surface with a drag mat during fall and spring seasons. It appears that the compost application did not shield the soil surface from evaporative losses or significantly modify the infiltration characteristics of the urban park soils. Nevertheless, no adverse effects of green waste compost were noted such that, under favourable economic conditions, it may serve as an alternative to traditional fertilizers.

5.2 | Sensitivity to type of irrigation application

Notable differences were found between sprinkler and flood irrigation practices in terms of the soil moisture conditions (Figures 3 and 7), dynamic water stress (Figures 9 and 10) and water balance partitioning (Figures 8 and 11). As a result, the type of irrigation was the dominant factor influencing the soil water balance model of the urban parks, consistent with the simplified irrigation scenarios of Volo et al. (2014). Sprinkler irrigation consisting of small, frequent events in the warm season result in lower soil moisture values, promote less leakage from the root zone, and contain a shorter period of high *ET* as compared to flood irrigation, at about half of the total outdoor water use (Table 6). However, sprinkler irrigation is more susceptible to the interannual variability of P such that dry conditions during warm and cool seasons can lead to high Θ that can impact turf grasses. Sprinkler

TABLE 7 Average dynamic water stress and leakage during cool and warm seasons for study parks under four irrigation scenarios corresponding to: (1) current schedule and magnitude of events, (2) an 18% reduction in irrigation input by magnitude, (3) a reduction in irrigation by changing warm season frequency and (4) a 30% reduction in irrigation input by magnitude

				Average Θ (–)		Average L (mm)	
Study Park	Irrigation scenario	Irrigation (mm/year)	Water conserved (%)	Cool season	Warm season	Cool season	Warm season
PV	1	766	0	0.46	0.29	0.74	0
	2	628	18	0.51	0.41	0.63	0
	3	620	19	0.46	0.45	0.74	0
	4	536	30	0.57	0.51	0.55	0
EN	1	1511	0	0.47	0.42	167.3	372.0
	2	1239	18	0.44	0.42	101.8	177.0
	3	1286	15	0.36	0.48	302.7	172.0
	4	1058	30	0.46	0.45	62.6	89.6

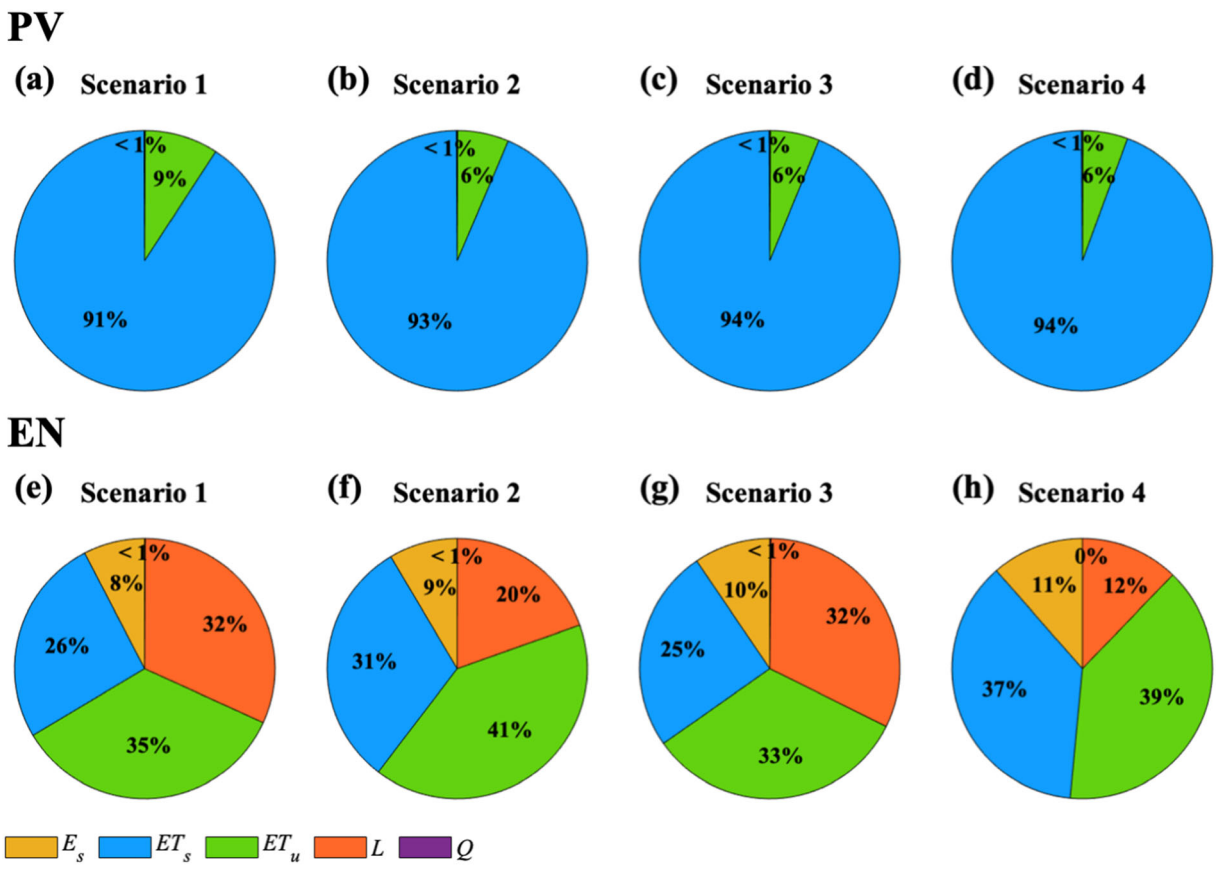

FIGURE 11 Annual water balance components for irrigation scenarios (1 through 4) for (a–d) PV and (e–h) EN study parks obtained over 15-year simulation periods

irrigation also leads to very low amounts of leakage in the cool season to support deep-rooted trees, whereas flood irrigation with its large, infrequent pulses can benefit surrounding trees during both seasons. A further consideration is that sprinkler irrigation will likely lead to lower heat reduction given the lower amounts of evaporative cooling.

5.3 | Water savings through irrigation scheduling

Long-term modelling scenarios showed the feasibility of reducing water use for both sprinkler and flood irrigation types. Since the model was tested with local observations of θ and ET and accounted for the interannual variability in P and ET_o, the scenarios are the best current representation of the fate of outdoor water within the upper soil profile of the study parks. While more advanced ecohydrological models are available for urban areas (e.g., Cristiano et al., 2020; Fatichi et al., 2016; Meili et al., 2020), the soil water balance approach of Laio et al. (2001) and Porporato et al. (2001) represented well the dominant role of the irrigation type and provided insights on the effects of changes in irrigation. Sprinkler and flood irrigation scenarios showed that the stakeholder target of an 18% reduction in water use could be achieved with low impacts on the soil water balance or plant stress, with further reductions of 30% also being feasible. The reduction of event size or magnitude for daily sprinkler or bi-weekly flood pulses had improved outcomes as compared to changes in the event frequency. This suggests that small changes in watering depth, while keeping the current timing, can have measurable benefits for urban parks in Phoenix, including lower biomass production and less leakage below the root zone.

6 | CONCLUDING REMARKS

This study utilized ecohydrological monitoring and modelling efforts in the context of an experimental manipulation in two urban parks. As such, it is considered an integrated study in ecohydrology that King and Caylor (2011) highlighted as needed for advancing the field, in particular for urban areas where less attention has been paid to date. By quantifying the effect of compost treatments in a real-world setting, we identified that water conservation targets could not be met unless irrigation scheduling was also altered. Small changes in watering depth under the current irrigation timing offer several benefits for urban park management, while minimizing the potential impacts to turf grass conditions. These outcomes were developed with the City of Phoenix Parks and Recreation Department and summarized in ways that highlighted the co-benefits for green waste compost applications with changes in irrigation management. Additional observations in urban areas (e.g., Alizadehtazi et al., 2020;

Gomez-Navarro et al., 2019; Vivoni et al., 2020) would certainly help elucidate further the fate of irrigation and other water sources. Furthermore, the incorporation of these findings in regional simulations (e.g., Reyes et al., 2018; Bohn et al., 2018; Wang, Vivoni, et al., 2021) would allow an assessment of the water savings potential at the city or metropolitan area scale. Similarly, it would be useful to determine the sensitivity of these outcomes to a broader set of rainfall scenarios, including changes to frequency and amount. As monitoring efforts of green infrastructure improve, urban ecohydrology models can offer the means to quantify spatiotemporal conditions and elucidate the underlying mechanisms driving the response to management decisions. The sensitivity of the study outcomes to the two forms of irrigation suggests that these results can be of broad utility for the management of urban parks.

ACKNOWLEDGEMENTS

We thank the City of Phoenix Parks and Recreation Department, in particular Larry Polk, Joel Carbajal and Rick Templeton, for their help in obtaining site permits and irrigation data, field support and for numerous discussions of the modelling outcomes in Encanto and Paradise Valley Parks. Project funding was provided by the Central Arizona Project, the City of Phoenix, and the Innovative Conservation Program of the Metropolitan Water District of Southern California. Planet imagery was made available through the Planet Incubator Program at Arizona State University. We are grateful to Bill Campbell and the Arizona State University Rob and Melani Walton Sustainability Solutions Service for their support. We thank Giuseppe Mascaro and Margaret Garcia for their comments on earlier versions of this work. We also thank the Arizona Meteorological Network (http://cals.arizona.edu/AZMET/) for providing weather station data. The data sets collected as part of this study at the two parks (Kindler & Vivoni, 2021) and the eddy covariance observations (Kindler et al., 2020) are available through Zenodo.

DATA AVAILABILITY STATEMENT

The data sets collected as part of this study at the two parks (Kindler and Vivoni, 2021) and the eddy covariance observations (Kindler et al., 2020) are available through Zenodo.

ORCID

Mercedes Kindler https://orcid.org/0000-0003-3798-6021
Enrique R. Vivoni https://orcid.org/0000-0002-2659-9459
Eli R. Pérez-Ruiz https://orcid.org/0000-0003-4954-0238
Zhaocheng Wang https://orcid.org/0000-0002-8154-9630

REFERENCES

Alizadehtazi, B., Gurian, P. L., & Montalto, F. A. (2020). Observed variability in soil moisture in engineered urban green infrastructure systems and linkages to ecosystem services. *Journal of Hydrology*, *590*, 125381. https://doi.org/10.1016/j.jhydrol.2020.125381

Balling, R. C., & Gober, P. (2007). Climate variability and residential water use in the city of Phoenix, Arizona. *Journal of Applied Meteorology and Climatology*, *46*(7), 1130–1137. https://doi.org/10.1175/JAM2518.1

Balling, R. C., Gober, P., & Jones, N. (2008). Sensitivity of residential water consumption to variations in climate: An intraurban analysis of Phoenix, Arizona. *Water Resources Research*, *44*, W10401. https://doi.org/10.1029/2007WR006722

Beard, J. B., & Green, R. L. (1994). The role of turfgrasses in environmental protection and their benefits to humans. *Journal of Environmental Quality*, *23*, 452–460. https://doi.org/10.2134/jeq1994.00472425002300030007x

Bohn, T. J., Vivoni, E. R., Mascaro, G., & White, D. D. (2018). Land and water use changes in the US-Mexico border region, 1992-2011. *Environmental Research Letters*, *13*(11), 114005. https://doi.org/10.1088/1748-9326/aae53e

Brown, P. W. (2005). *Standard reference evapotranspiration: A new procedure for estimating reference evapotranspiration in Arizona*. Cooperative Extension Publication AZ1324, University of Arizona. 12 pp

Brown, P. W., & Kopec, D. (2014). *Converting reference evapotranspiration into turf water use*. AZ1195, The University of Arizona. 5 pp

Brown, P. W., Mancino, C. F., Young, M. H., Thompson, T. L., Wierenga, P. J., & Kopec, D. M. (2001). Penman Monteith crop coefficients for use with desert turf systems. *Crop Science*, *41*, 1197–1206. https://doi.org/10.2135/cropsci2001.4141197x

Buch, R., O'Neill, D., Lubenow, C., DeFilippis, M., & Dalrymple, M. (2018). Collaboration for regional sustainable circular economy innovations. In S. Dhiman & J. Marques (Eds.), *Handbook of engaged sustainability* (Vol. 2-2) (pp. 703–728). Springer. https://doi.org/10.1007/978-3-319-71312-0_24

Buyantuyev, A., Wu, J., & Gries, C. (2007). Estimating vegetation cover in an urban environment based on Landsat ETM+imagery: A case study in Phoenix, USA. *International Journal of Remote Sensing*, *28*(2), 269–291. https://doi.org/10.1080/01431160600658149

Caylor, K. K., Manfreda, S., & Rodríguez-Iturbe, I. (2005). On the coupled geomorphological and ecohydrological organization of river basins. *Advances in Water Resources*, *28*, 69–86. https://doi.org/10.1016/j.advwatres.2004.08.013

Chen, J., Jönsson, P., Tamura, M., Gu, Z., Matsushita, B., & Eklundh, L. (2004). A simple method for reconstructing a high-quality NDVI time-series data set based on the Savitzky-Golay filter. *Remote Sensing of Environment*, *91*, 332–344. https://doi.org/10.1016/j.rse.2004.03.014

Chow, W. T. L., Volo, T. J., Vivoni, E. R., Jenerette, C. D., & Ruddell, B. L. (2014). Seasonal dynamics of a suburban energy balance in Phoenix, Arizona. *International Journal of Climatology*, *34*(15), 3863–3880. https://doi.org/10.1002/joc.3947

Coker, C. (2017). Phoenix composting facility rises from desert floor. *BioCycle*, *58*(9), 17–20.

Cristiano, E., Deidda, R., & Viola, F. (2020). EHSMu: A new ecohydrological streamflow model to estimate runoff in urban areas. *Water Resources Management*, *34*(15), 4865–4879. https://doi.org/10.1007/s11269-020-02696-0

Duan, Q. Y., Gupta, V. K., & Sorooshian, S. (1993). Shuffled complex evolution approach for effective and efficient global minimization. *Journal of Optimization Theory and Applications*, *76*, 501–521. https://doi.org/10.1007/BF00939380

Fatichi, S., Vivoni, E. R., Ogden, F. L., Ivanov, V. Y., Mirus, B., Gochis, D., Downer, C. W., Camporese, M., Davidson, J. H., Ebel, B., Jones, N., Kim, J., Mascaro, G., Niswonger, R., Restrepo, P., Rigon, R., Shen, C., Sulis, M., & Tarboton, D. (2016). An overview of current applications, challenges and future trends of distributed process-based models in hydrology. *Journal of Hydrology*, *537*, 45–60. https://doi.org/10.1016/j.jhydrol.2016.03.026

Fuentealba, M. P., Zhang, J., Kenworthy, K. E., Erickson, J. E., Kruse, J., & Trenholm, L. E. (2015). Root development and profile characteristics of bermudagrass and zoysiagrass. *HortScience*, *50*(10), 1429–1434. https://doi.org/10.21273/HORTSCI.50.10.1429

Garfin, G., Franco, G., Blanco, H., Comrie, A., Gonzalez, P., Piechota, T., Smyth, R., & Waskom, R. (2014). Ch. 20: Southwest. In J. M. Melillo, T. C. Richmond, & G. W. Yohe (Eds.), *Climate change impacts in the United States: The third national climate assessment* (pp. 462–486). U.S. Global Change Research Program.

Gleick, P. H. (2010). Roadmap for sustainable water resources in southwestern North America. *Proceedings of the National Academy of Sciences*, *107*(50), 21300–21305. https://doi.org/10.1073/pnas.1005473107

Gober, P., Brazel, A., Quay, R., Myint, S., Grossman-Clarke, S., Miller, A., & Rossi, S. (2010). Using watered landscapes to manipulate urban heat island effects: How much water will it take to cool Phoenix? *Journal of the American Planning Association*, *76*(1), 109–121. https://doi.org/10.1080/01944360903433113

Gomez-Navarro, C., Pataki, D. E., Bowen, G. J., & Oerter, E. J. (2019). Spatiotemporal variability of water sources in urban soils and trees in the semiarid, irrigated Salt Lake Valley. *Ecohydrology*, *12*(8), e2154. https://doi.org/10.1002/eco.2154

Grimm, N. B., Foster, D., Groffman, P., Grove, J. M., Hopkinson, C. S., Nadelhoffer, K., Peters, D., & Pataki, D. E. (2008). The changing landscape: Ecosystem. Responses to urbanization and pollution across climatic and societal gradients. *Frontiers in Ecology and the Environment*, *6*, 264–272. https://doi.org/10.1890/070147

Hirt, P., Gustafson, A., & Larson, K. L. (2008). The mirage in the valley of the sun. *Environmental History*, *13*, 248–514. https://doi.org/10.1093/envhis/13.3.482

Kindler, M. (2021), Water conservation potential of turfgrass irrigation management in urban parks. Master of Science in Civil, Environmental and Sustainable Engineering. Arizona State University, 191 pp.

Kindler, M., Pérez-Ruiz, E. R., Wang, Z., and Vivoni, E. R. (2020), Water, energy and carbon fluxes and ancillary meteorological and remote sensing measurements at Encanto Golf Course, Phoenix, Arizona during 2019-2020. https://doi.org/10.5281/zenodo.3872381

Kindler, M., and Vivoni, E. R. (2021), Precipitation, soil water content and reference evapotranspiration at two urban parks in Phoenix, Arizona during 2018-2020. https://doi.org/10.5281/zenodo.4783588

King, E. G., & Caylor, K. K. (2011). Ecohydrology in practice: Strengths, conveniences, and opportunities. *Ecohydrology*, *4*, 608–612. https://doi.org/10.1002/eco.248

Laio, F., Porporato, A., Ridolfi, L., & Rodríguez-Iturbe, I. (2001). Plants in water-controlled ecosystems: Active role in hydrologic processes and response to water stress II. Probabilistic soil moisture dynamics. *Advances in Water Resources*, *24*, 707–723. https://doi.org/10.1016/S0309-1708(01)00005-7

Larson, E. K., Casagrande, D., Harlan, S. L., & Yabiku, S. T. (2009). Residents' yard choices and rationales in a desert city: Social priorities, ecological impacts, and decision tradeoffs. *Environmental Management*, *44*(5), 921–937. https://doi.org/10.1007/s00267-009-9353-1

Larson, E. K., Hoffman, J., & Ripplinger, J. (2017). Legacy effects and landscape choices in a desert city. *Landscape and Urban Planning*, *165*, 22–29. https://doi.org/10.1016/j.landurbplan.2017.04.014

Larson, E. K., & Perrings, C. (2013). The value of water-related amenities in an arid city: The case of the Phoenix metropolitan area. *Landscape and Urban Planning*, *109*, 45–55. https://doi.org/10.1016/j.landurbplan.2012.10.008

Manfreda, S., Scanlon, T. M., & Caylor, K. K. (2010). On the importance of accurate depiction of infiltration processes on modeled soil moisture and vegetation water stress. *Ecohydrology*, *3*, 155–165. https://doi.org/10.1002/eco.79

Martin, C. A. (2008). Landscape sustainability in a Sonoran Desert city. *Cities and the Environment*, *1*(2), 1–16. https://doi.org/10.15365/cate.1252008

Mascaro, G. (2017). Multiscale spatial and temporal statistical properties of rainfall in central Arizona. *Journal of Hydrometeorology*, *18*(1), 227–245. https://doi.org/10.1175/JHM-D-16-0167.1

McDonald, G. M. (2010). Water, climate change, and sustainability in the southwest. *Proceedings of the National Academies of Sciences*, *107*(50), 21256–21262. https://doi.org/10.1073/pnas.0909651107

Meili, N., Manoli, G., Burlando, P., Bou-Zeid, E., Chow, W. T. L., Coutts, A. M., Daly, E., Nice, K. A., Roth, M., Tapper, N. J., Velasco, E., Vivoni, E. R., & Fatichi, S. (2020). An urban ecohydrological model to quantify the effect of vegetation on urban climate and hydrology (UT&C v1.0). *Geoscientific Model Development*, *13*, 335–362. https://doi.org/10.5194/gmd-13-335-2020

Milesi, C., Running, S. W., Elvidge, C. D., Dietz, J. B., Tuttle, B. T., & Nemani, R. R. (2005). Mapping and modeling the biogeochemical cycling of turf grasses in the United States. *Environmental Management*, *36*(3), 426–438. https://doi.org/10.1007/s00267-004-0316-2

Pataki, D. E., Boone, C. G., Hogue, T. S., Jenerette, G. D., McFadden, J. P., & Pincetl, S. (2011). Socio-ecohydrology and the urban water challenge. *Ecohydrology*, *4*, 341–347. https://doi.org/10.1002/eco.209

Pérez-Ruiz, E. R., Vivoni, E. R., & Templeton, N. P. (2020). Urban land cover type determines the sensitivity of carbon dioxide fluxes to precipitation in Phoenix, Arizona. *PLoS ONE*, *15*(2), e0228537. https://doi.org/10.1371/journal.pone.0228537

Planet Team. (2017), Planet application program interface: In space for life on earth. San Francisco, CA. https://api.planet.com

Porporato, A., Laio, F., Ridolfi, L., Caylor, K. K., & Rodríguez-Iturbe, I. (2003). Soil moisture and plant stress dynamics along the Kalahari precipitation gradient. *Journal of Geophysical Research*, *108*(D3), 4127. https://doi.org/10.1029/2002JD002448

Porporato, A., Laio, F., Ridolfi, L., & Rodríguez-Iturbe, I. (2001). Plants in water-controlled ecosystems: Active role in hydrologic processes and response to water stress III. Vegetation water stress. *Advances in Water Resources*, *24*, 725–744. https://doi.org/10.1016/S0309-1708(01)00006-9

Quesnel, K. J., Ajami, N., & Marx, A. (2019). Shifting landscapes: Decoupled urban irrigation and greenness patterns during severe drought. *Environmental Research Letters*, *14*, 064012. https://doi.org/10.1088/1748-9326/ab20d4

Reyes, B., Houge, T., & Maxwell, R. (2018). Urban irrigation suppresses land surface temperature and changes the hydrologic regime in semi-arid regions. *Water*, *10*, 1563. https://doi.org/10.3390/w10111563

Robbins, P., & Sharp, J. T. (2003). Producing and consuming chemicals: The moral economy of the American lawn. *Economic Geography*, *79*(4), 425–451. https://doi.org/10.1111/j.1944-8287.2003.tb00222.x

Rodríguez-Iturbe, I., & Porporato, A. (2004). *Ecohydrology of water-controlled ecosystems: Soil moisture and plant dynamics* (p. 442). Cambridge University Press. https://doi.org/10.1017/CBO9780511535727

Templeton, N. P., Vivoni, E. R., Wang, Z.-H., & Schreiner-McGraw, A. P. (2018). Quantifying water and energy fluxes over different urban land covers in Phoenix, Arizona. *Journal of Geophysical Research*, *123*, 2111–2128. https://doi.org/10.1002/2017JD027845

Templeton, R. C., Vivoni, E. R., Méndez-Barroso, L. A., Pierini, N. A., Anderson, C. A., Rango, A., Laliberte, A. S., & Scott, R. L. (2014). High-resolution characterization of a semiarid watershed: Implications on evapotranspiration estimates. *Journal of Hydrology*, *509*, 306–319. https://doi.org/10.1016/j.jhydrol.2013.11.047

Vico, G., & Porporato, A. (2010). Traditional and micro-irrigation with stochastic soil moisture. *Water Resources Research*, *46*(3), W03509. https://doi.org/10.1029/2009WR008130

Vico, G., & Porporato, A. (2011a). From rainfed agriculture to stress-avoidance irrigation: I. A generalized irrigation scheme with stochastic soil moisture. *Advances in Water Resources*, *34*(2), 263–271. https://doi.org/10.1016/j.advwatres.2010.11.010

Vico, G., & Porporato, A. (2011b). From rainfed agriculture to stress-avoidance irrigation: II. Sustainability, crop yield, and profitability. *Advances in Water Resources*, *34*(2), 272–281. https://doi.org/10.1016/j.advwatres.2010.11.011

Vivoni, E. R., Kindler, M., Wang, Z., & Pérez-Ruiz, E. R. (2020). Abiotic mechanisms drive enhanced evaporative losses under urban oasis conditions. *Geophysical Research Letters*, *47*, e2020GL090123. https://doi.org/10.1029/2020GL090123

Volo, T. J., Vivoni, E. R., Martin, C. A., Earl, S., & Ruddell, B. L. (2014). Modelling soil moisture, water partitioning and plant water stress under irrigated conditions in desert urban areas. *Ecohydrology*, *7*, 1297–1313. https://doi.org/10.1002/eco.1457

Volo, T. J., Vivoni, E. R., & Ruddell, B. L. (2015). An ecohydrological approach to conserving urban water through optimized landscape irrigation schedules. *Landscape and Urban Planning*, *133*, 127–132. https://doi.org/10.1016/j.landurbplan.2014.09.012

Wang, C., Turner, V. K., Wentz, E. A., Zhao, Q., & Myint, S. W. (2021). Optimization of residential green space for environmental sustainability and property appreciation in metropolitan Phoenix, Arizona. *Science of the Total Environment*, *763*, 144605. https://doi.org/10.1016/j.scitotenv.2020.144605

Wang, Z., Vivoni, E. R., Bohn, T. J., & Wang, Z.-H. (2021). A multiyear assessment of irrigation cooling capacity in agricultural and urban settings of central Arizona. *Journal of the American Water Resources Association*, *57*(5), 771–788. https://doi.org/10.1111/1752-1688.12920

Weindorf, D. C., Zartman, R. E., & Allen, B. L. (2006). Effect of compost on soil properties in Dallas, Texas. *Compost Science & Utilization*, *14*, 59–67. https://doi.org/10.1080/1065657X.2006.10702264

Whitney, K. M., Vivoni, E. R., Duniway, M., Bradford, J., Reed, S. C., & Belnap, J. (2017). Ecohydrological role of biological soil crusts across a gradient in levels of development. *Ecohydrology*, *10*(7), e1875. https://doi.org/10.1002/eco.1875

Yabiku, S. T., Casagrande, D. G., & Farley-Metzger, E. (2008). Preferences for landscape choice in a southwestern desert city. *Environment and Behavior*, *40*(3), 382–400. https://doi.org/10.1177/0013916507300359

Zemánek, P. (2011). Evaluation of compost influence on soil water retention. *Acta Universitatis Agriculturae et Silviculturae Mendelianae Brunensis*, *59*(3), 227–232. https://doi.org/10.11118/actaun201159030227

How to cite this article: Kindler, M., Vivoni, E. R., Pérez-Ruiz, E. R., & Wang, Z. (2022). Water conservation potential of modified turf grass irrigation in urban parks of Phoenix, Arizona. *Ecohydrology*, e2399. https://doi.org/10.1002/eco.2399